

# EVALUATION OF WAVELET TRANSFORM BASED FEATURE EXTRACTION TECHNIQUES FOR DETECTION AND CLASSIFICATION OF FAULTS ON TRANSMISSION LINES USING WAMS DATA

Ani HARISH<sup>1,2</sup> , Prince ASOK<sup>1,2</sup> , Jayan Madasseril VASUDEVAN<sup>1</sup> 

<sup>1</sup>APJ Abdul Kalam Technological University,  
CET Campus, 695016 Thiruvananthapuram, India

<sup>2</sup>Department of Electrical Engineering, Rajiv Gandhi Institute of Technology,  
Velloor PO, 686501 Kottayam, India

ani.ramachandran@rit.ac.in, prince@rit.ac.in, jayanmadasseri@gmail.com

DOI: 10.15598/aeec.v20i4.4664

Article history: Received Aug 11, 2022; Revised Sep 28, 2022; Accepted Oct 02, 2022; Published Dec 31, 2022.  
This is an open access article under the BY-CC license.

**Abstract.** *The smart grid is an intelligent power system network that should be reliable and resilient for sustainable operation. Wide-Area Measurement Systems (WAMS) are deployed in the power grid to provide real-time situational awareness to the power grid operators. An excellent strategy for exploiting the WAMS data effectively is to extract relevant insights from the increasing volume of data collected. Feature extraction techniques are pivotal in developing data-driven models for power systems. This paper proposes an ensemble feature extraction method for developing intelligent data-driven models for transmission line fault detection and classification. A comparative efficacy analysis of the proposed ensemble feature extraction method is carried out with state-of-the-art feature extraction methods. The models developed and evaluated with the feature data derived with the proposed method give an accuracy of 100 % for fault detection and 99.78 % for fault classification. This method also has the advantage of significantly reducing training and testing time. Features are extracted from the WAMS data collected by simulating an IEEE 39 bus test system in the PowerWorld simulator.*

**grid, transmission lines, WAMS, wavelet transform.**

## 1. Introduction

Power delivery networks worldwide are becoming smarter with the deployment of intelligent systems. A smart grid is an intelligent, reliable, resilient, and sustainable power system network [1]. Phasor Measurement Units (PMUs) are a feature of modern power grids that collect GPS synced data. A sizable amount of Wide-Area Measurement Systems (WAMS) data is recorded and saved with PMU installations on the power network. This growing body of data can yield insightful conclusions. Algorithms for data mining or machine learning aid in the information extraction process [3]. Relay malfunctions are frequently reported due to the growing use of power electronics and distributed energy sources on the electrical grid [4]. Most recorded blackouts are due to the cascading effects of the primary protection system failure [6].

Transmission Line protection is a vital aspect of a resilient and self-healing smart grid [2]. Intelligent fault diagnosis methods are critical for achieving a reliable smart grid. Wide Area situational awareness plays a pivotal role in improving the resiliency and reliability of the grid [1]. Methods for detecting, classifying, and localising transmission line faults in

## Keywords

**Fault classification, fault detection, feature extraction techniques, machine learning, smart**

the literature typically fall into one of two categories: physics model-based or data-driven model-based [5]. In power grids, stochastic renewable energy sources are becoming more prevalent, making it hard to develop a solid mathematical system model [5]. The reliability of model-based methods has thus become questionable. Intelligent approaches that extract information from measurement data are best suited for developing protective solutions for the present power system. Short circuit faults on transmission lines can be found, located, and categorised using data mining techniques using WAMS data [3].

Features are representations of the input data and contain the characteristics of and information about the input data. To build machine learning models for Fault Detection and Classification (FD&C), feature extraction techniques are important. With the help of feature extraction techniques, pertinent information may be extracted from power system signal data for FD&C as well as essential patterns can be found in measurement data to create machine learning models. Signal processing techniques, wavelet transform, wavelet multivariate analysis, and wavelet entropy analysis are the most applied feature extraction methods [7], [8], [9] and [10] for FD&C in transmission lines. Some other signals processing techniques for power system signals analysis are Fourier transform, Stockwell transform and Hilbert Huang transform [11], [12] [13] and [14]. Wavelet transform gives good resolution in both the time and frequency domains [15] and [16] and is used predominantly in the literature for power signals analysis.

Authors in [18] propose a transmission line protection scheme using Discrete Wavelet Transform Multi-Resolution Analysis (DWT-MRA) of current signals. The energy values of the approximation coefficients of the current signals are used to categorise faults. In [19], the authors propose fault detection and classification of transmission lines using a double channel extreme learning machine. The feature dataset is formed from the energy values of the DWT coefficients at each level and the standard deviation of the coefficient values. The three phase voltage and current signals from both ends of a transmission line are analysed. In [7], authors propose Wavelet Entropy values of the voltage signals as inputs to an Artificial Neural Network (ANN) for fault type classification. Reference [20] proposes transmission line fault classification using DWT feature extraction. DWT coefficients using db6 mother wavelet with level 6 decomposition of three-phase current signals form the features. An ANN with the sum of the level 6 detail coefficients as inputs does the fault type classification. In [21], the authors propose a feature extraction using Wavelet Packet Entropy and ANN for faults classification. The Mother wavelet chosen is db6 with three levels of decomposition. Features are

the Wavelet Packet decomposition of three-phase fault current signals from the faulted line. Reference [22] proposes a similar approach as [20] for feature extraction. [23] presents the Maximum Overlap Discrete Wavelet Transform (MODWT) for feature extraction. The energy values of the MODWT coefficients form the features. In [24] and [25] Decision Tree (DT) and Ensemble Tree Classifier (BTEC) algorithms are used for classification. [8] presents fault classification by K Nearest Neighbour (KNN) algorithm. The instantaneous values of three-phase currents are the inputs to the classification algorithm. Authors use the Support Vector Machine (SVM) classification algorithm in [11] as the faults classifier. Reference [26] proposes an ensemble feature extraction method using wavelet transform.

### 1.1. Related Work

WAMS data collected by PMUs is GPS synchronised and offers a broad system view that can be used to create FD&C models. In [11], the researchers provide a method for classifying and recognising faults based on PMU data. Park and Fast Fourier Transformation techniques are used to extract the features, and SVM is used to categorise the faults. In [18], researchers suggest creating FD&C models for transmission line protection using the wavelet decomposition's energy as attributes taken from the WAMS data. The authors of [27] employ PMU data to identify and classify various power grid events. In [28] the authors propose a novel method for detecting faults using the direction of active and reactive power flow on each side of the line. The algorithm presented has fault classification capability, but the time taken to classify the faults is not mentioned. In reference [29] authors propose fault detection and location by a methodology constructing a nodal admittance matrix. Knowledge of network parameters and topology is required for constructing the nodal admittance matrix. Reference [30] proposes the detection of high impedance faults in a solar photovoltaic integrated system. The energy values of the wavelet coefficients are extracted as features and the faults are classified using the LSTM network with an accuracy of 92.42 %. In [31], features are extracted from the PMU data using phaselet transform, and faults are classified by the Gaussian Naive Bayes (GNB) algorithm.

A few works that demonstrate FD&C models created using WAMS data are references [11], [18], [27] and [31]. Most of the machine learning methods for developing FD&C models for detecting, classifying, and localizing faults on transmission lines use the wavelet transform based feature extraction techniques [7], [8], [9], [10], [12], [18], [19], [20], [21], [22], [23], [24], [25] and [30]. Hence, there is a need to identify

a computationally efficient wavelet transform-based feature extraction method for developing FD&C models for FD&C on transmission lines using WAMS data.

### 1.2. Contribution

The main contributions of this research work are:

- This paper investigates wavelet transform based feature extraction techniques for developing FD&C models for transmission lines using WAMS data. The time taken for feature extraction, the training and testing time of the FD&C models and the accuracy are the performance measures considered for determining the efficacy of the feature extraction techniques.
- An ensemble feature extraction method is developed. The performance of the classification models developed with state-of-the-art classifier methods are evaluated with the ensemble features data derived from complete, sparse, and noisy measurement data to validate the efficacy of the features.

### 1.3. Structure of the Paper

The structure of this paper is as follows. Section 2. gives a preview of the wavelet transform feature extraction methods used in this paper. Section 3. describes the experimental setup for simulation and the feature data set development for fault detection and classification. Section 4. has the results and the discussion. Section 5. has the concluding remarks.

## 2. Feature Extraction Techniques

The different feature extraction techniques used in this paper are the Discrete Wavelet Transform (DWT), Wavelet Packet Transform (WPT), Maximum Overlap Discrete Wavelet Transform (MODWT) and Wavelet Scattering Transform (WST). Multi-resolution analysis of the signals is done by decomposition using DWT, WPT, MODWT and WST. Statistical features of the wavelet coefficients, energy levels of the decomposition coefficients, and entropy values are also derived as features.

### 2.1. Discrete Wavelet Transform

Wavelet transform is a signal processing technique used for analyzing the signals in time and frequency

domains [15]. Wavelet transforms give good time resolution and frequency resolution for high frequency and low-frequency events. Continuous Wavelet Transforms (CWT) are used for wavelet analysis of continuous signals and Discrete Wavelet Transforms (DWT) for discrete signals. DWT helps in the multilevel decomposition of the signal. The signal’s frequency band is resolved into low (approximation) and high (detail coefficients) components using high and low pass filters at different levels. The operation is repeated by inputting the down-sampled low pass component into another filter pair. The approximation coefficients are the low-frequency decomposition, and the detail coefficients are the signal’s high-frequency decomposition.

A discrete signal  $S_n(n)$  can be represented as in Eq. (1), where  $\mu_{j_0,k}[n]$  and  $\omega_{j,k}[n]$  are discrete functions that are orthogonal to each other:

$$S_n[n] = \frac{1}{\sqrt{N}} \sum_k V_\mu[j_0, k] \mu_{j_0,k}[n] + \sum_{j=j_0}^{\infty} \sum_k V_\omega[j, k] \omega_{j,k}[n]. \tag{1}$$

The wavelet coefficients can be represented as the approximation coefficients as in Eq. (2), and the detail coefficients as in Eq. (3):

$$V_\mu[j_0, k] = \frac{1}{\sqrt{N}} \sum_n S_n[n] \mu_{j_0,k}[n], \tag{2}$$

$$V_\omega[j, k] = \frac{1}{\sqrt{N}} \sum_n S_n[n] \omega_{j,k}[n]. \tag{3}$$

The wavelet decomposition at three levels is as shown in Fig. 1. The low pass and high pass filters decompose the signal, and the output of the filters are down-sampled to get the approximation and detail coefficients. Only the output of the low pass filter is decomposed again at subsequent levels.

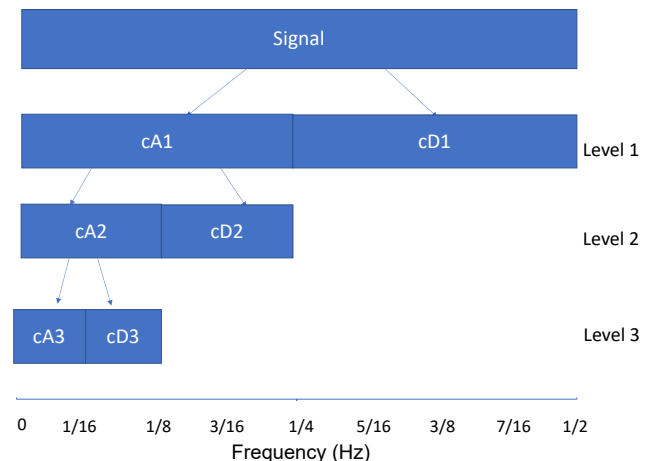


Fig. 1: Wavelet decomposition at level 3.

## 2.2. Wavelet Packet Transform

The WPT divides the frequency into equal bands at each level [17]. In WPT, both the outputs of the low pass filter and high pass filters are further decomposed in the subsequent levels. The wavelet packet decomposition for three levels is shown in Fig. 2. WPT gives a better frequency resolution than DWT.

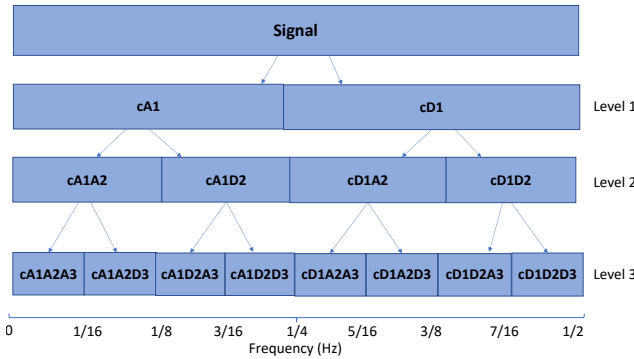


Fig. 2: Wavelet Packet Transform decomposition at level 3.

## 2.3. Maximum Overlap Discrete Wavelet Transform

Lowpass and highpass filters are applied to the input signal at each level in the Maximal Overlap Discrete Wavelet Transform (MODWT), which is comparable to the Discrete Wavelet Transform (DWT) [32]. The MODWT does not decimate the coefficients, and at every level of the transform, the number of wavelets and scaling coefficients is equal to the number of sample observations. MODWT does not downsample the output at each scale. The MODWT is also known as non-decimated DWT, stationary DWT, translation invariant DWT, and time-invariant DWT due to this.

## 2.4. Wavelet Scatter Transform

Wavelet Scatter Transform (WST) provides strong time and frequency localization and is impervious to translations. It preserves high frequency information for classification and is akin to Convolutional Neural Networks (CNN) [33]. The advantage WST has over CNN is of lesser training time and a smaller dataset [34].

Let  $w(t)$  be the signal,  $\phi_K(t)$  be the low pass filter and  $\Psi_K$  be the wavelet. A locally translational invariant of the signal  $w(t)$  can be obtained by the convolution of  $w(t)$  and  $\phi_K(t)$ ,  $S_{0t} = \phi_K(t) * w(t)$  [35]. The wavelet modulus transform recovers the high frequency components.

$$|\mu_1|w = \{S_{0t}, |w * \Psi_{K_1}(t)|\}. \quad (4)$$

The first order wavelet scattering coefficients can be obtained by Eq. (5):

$$S_{1t}w(t) = \{|w * \Psi_{K_1}| * \phi_K(t)\}. \quad (5)$$

The second order coefficients can be obtained by Eq. (6):

$$S_{2t}w(t) = \{||w * \Psi_{K_1}| * \Psi_{K_2}| * \phi_K(t)\}. \quad (6)$$

Thus the  $m$ -th order scattering coefficients can be obtained by Eq. (7):

$$S_{mt}w(t) = \{||w * \Psi_{K_1} * \dots * \Psi_{K_m}| * \phi_K(t)\}. \quad (7)$$

The final scattering matrix aggregates the scattering coefficients of all orders to form the features of the input signal.

## 3. Data Acquisition, Feature Extraction, Fault Detection and Classification

Figure 7 illustrates the feature extraction and FD&C process flow.

### 3.1. WAMS Based Data Acquisition

The IEEE 39 bus test system model was simulated in the PowerWorld Simulator [36]. IEEE 39 bus test system is a 10 generator, 39 bus system with 34 lines and 12 transformers with a nominal voltage of 345 kV and system frequency of 60 Hz. Figure 3 shows the one-line diagram of the test system.

The parameters for the test system model are from [36].

To simulate faults in the IEEE 39 bus test system, the PowerWorld Simulator's Transient stability module was utilised. Case studies were conducted for no fault, Single Line to Ground fault (LG), Line to Line (LL), Line to Line to Ground (LLG), and balanced (LLL) faults. Signals, voltage, voltage angle, and current are recorded by varying the fault resistance between 1–50 in steps of 5  $\Omega$  and fault locations on the transmission line in steps of 10 % from 10 to 90. The parameters for the various fault cases considered are listed in Tab. 1. For example, an LG fault was inserted on the line connecting buses 2 and 25 at 70 % of the line length at 1 s and cleared at 1.03 s with a resistance of 10  $\Omega$ . A LL fault was inserted on the line between buses 3 and 18 at 80 % of the line length at 1 s and cleared at 1.03 s with a resistance of 50  $\Omega$ . An LLG Fault was inserted on the line between buses 21 and 22 at 1 s at 40 % of the line length from bus 21 and cleared after 1.03 s

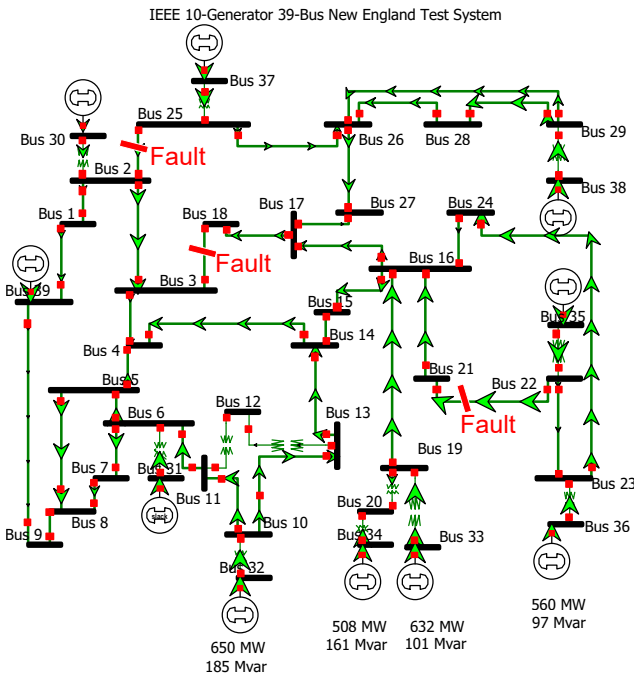


Fig. 3: IEEE 39 bus test system.

with a resistance of 50 Ω. A LLL fault was inserted on the line between buses 21 and 22 at 40 % of the line length from bus 21 at 1 s and cleared at 1.03 s with a resistance of 50 Ω. The simulation was run for 5 s for all the fault cases. The variations of the voltage, voltage angle, frequency, and current measurements for the above fault types are as shown in Fig. 5 and Fig. 6.

Tab. 1: Parameters for fault dataset generation.

Parameters	Values
Fault type	No-fault, LG, LL, LLG, LLL
Fault resistance (Ω)	1, 5, 10, 15, 20, 25, 35, 40, 50
Fault location (% of the length of the line)	10, 20, 30, 40, 50, 60, 70, 80, 90

During every simulation run, the PowerWorld Simulator’s dynamic simulator generated IEEE C37.118.2011 compliant messages, which were collected by the OpenPDC. These messages are stored in the Historian database of OpenPDC. The data was extracted from the OpenPDC Historian database as .csv files and then verified for discrepancies, cleaned, labelled, and imported into MATLAB. The setup for WAMS data acquisition is illustrated in Fig. 4.

The created data set contains 24,654 voltage, voltage-angle, current, current-angle, and frequency signal samples from the 39 buses. The generated dataset was divided into a training data set with 15,317 samples and a testing data set with 7134 samples in a 70 : 30 ratio.

Tab. 2: Distribution of data across classes in the data set for detecting faults.

Data set	No-fault (1)	Fault (2)
Training	3868	11,449
Testing	2229	4905

Tab. 3: Distribution of data for different fault types in the data set for classifying the faults.

Data set	NF (1)	LG (2)	LL (3)	LLG (4)	LLL (5)
Training	3868	2694	2694	2694	3367
Testing	2229	1154	1154	1154	1443

### 3.2. Feature Extraction

Features are specific characteristics of the input data. Many studies on power system data fault analysis have advocated Wavelet transforms as the most efficient feature extraction technique for power signal data [7], [8], [9], [10], [18], [19], [20], [21], [22] and [23]. For signal data transformation, we used the Discrete Wavelet Transform (DWT). Using the Daubechies Db4 mother wavelet, the signals were resolved into five levels of wavelet coefficients. The following methods were used to extract the features:

- The statistical characteristics of the wavelet decomposition of the signal data, such as standard deviation, range, Root Mean Square value (RMS), and crest factor. (Waveletstat feature dataset).
- Wavelet Entropy: consists of the entropy values of the signal data set’s wavelet coefficients determined using Eq. (8). Shannon Entropy is a measure of the quantity of information in a variable. Equation (8) is used to calculate the entropy of the wavelet coefficients at level  $j$ :

$$WET_t = \sum_{t=1}^{L_t} ps_{t,k} \cdot \log(ps_{t,k}), \quad (8)$$

where  $L_t$  is the number of coefficients in the  $t$ -th level and  $ps_{t,k}$  normalized squares of the wavelet coefficients at the  $t$ -th level.

- Wavelet Energy: The energy (L2 norm) of each wavelet decomposition at each level is included in this feature set. The energy of the wavelet decomposition are computed as follows in Eq. (9):

$$WEE = \|ApC\|^2 + \|DtC\|^2, \quad (9)$$

where ApC is the output of the low pass filter, and DtC is the output of the high pass filter at the different levels.

- Wavelet Packet Energy: Features are the energy of wavelet packet coefficients for wavelet packet tree nodes. This is the sum of the energies (squared L2 norms) for each level of wavelet packets.

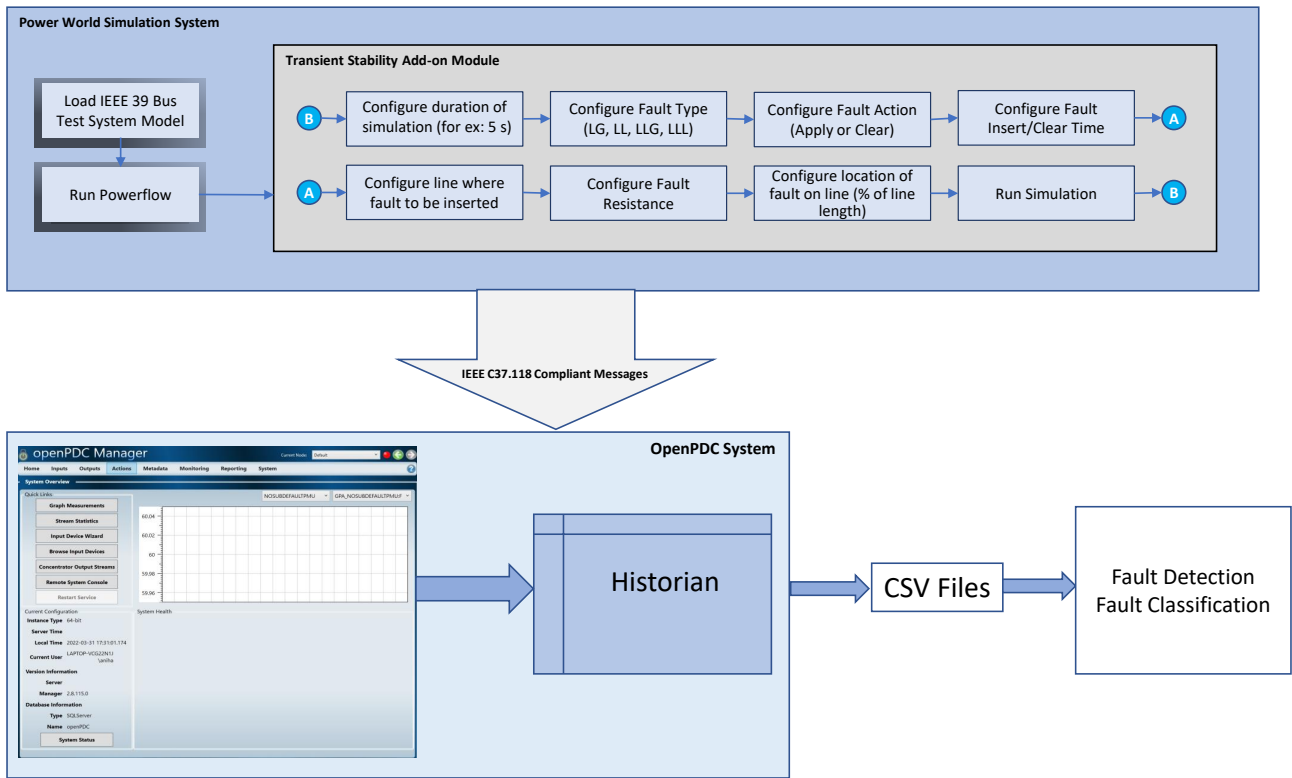


Fig. 4: Simulation setup for dataset generation.

- Wavelet Packet Entropy: Shannon entropy values of the wavelet packet coefficients for the wavelet packet tree nodes.
  - MODWT Energy: Energy of the MODWT coefficients at different levels:
- $$MEE = \|\text{modwtcoef}\|^2. \quad (10)$$
- Wavelet Scattering Transform (WST): WST coefficients for the input signal with an invariance scale of 1 are derived as the features.

### 3.3. Ensemble Feature Extraction

The wavelet energy, wavelet entropy, and statistical features of wavelet coefficients are used to develop the following ensemble feature extraction methods.

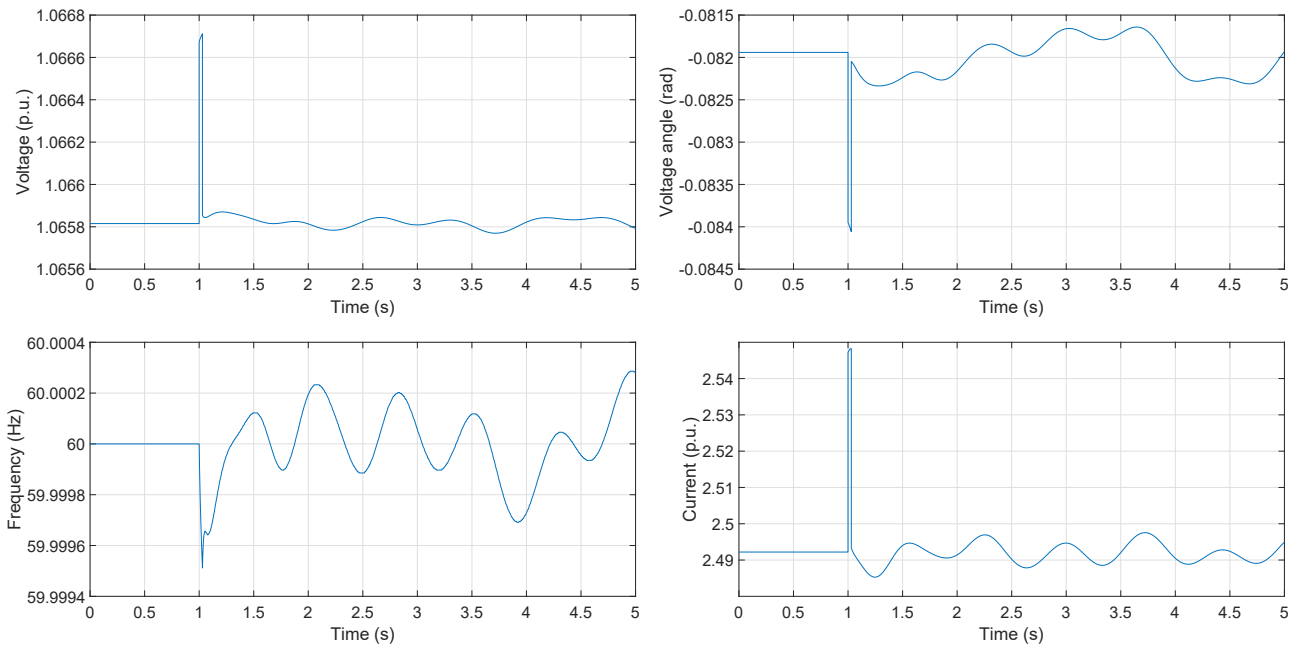
- Ensemblestatwentropy: An ensemble of statistical features and entropy values of the wavelet decomposition of signals.
- Ensemblestatwenergy: An ensemble of statistical features and energy values of the wavelet decomposition of signals.
- Ensemblestatwenergywentropy: An ensemble of statistical features, entropy, and energy of the wavelet coefficients.

### 3.4. Fault Detection and Classification

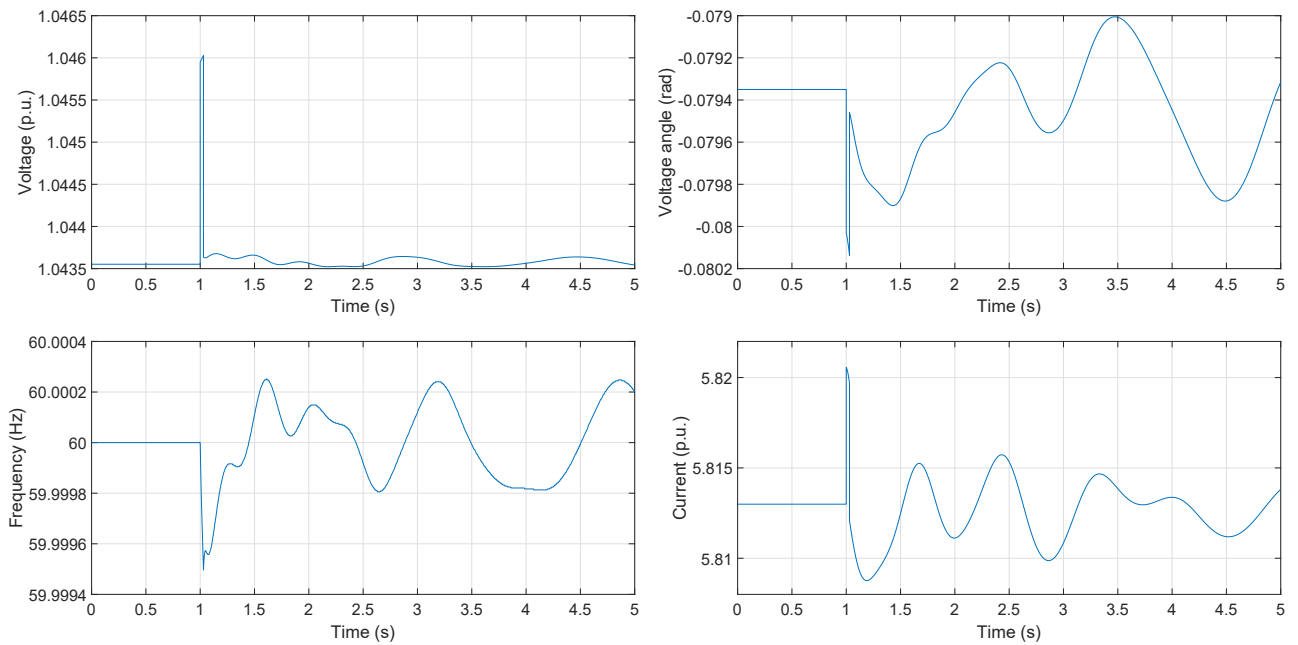
The identification of faults is a binary classification issue with two classes: no-fault (class 1) and fault (class 2). As indicated in Tab. 2, the fault detection models were trained using the training data set, and the performance of the detection models was evaluated using the testing data set. Classification of faults is a multi-class classification task. The distinct categories in the data set include No-Fault (NF), Line-to-Ground fault (LG), Line-to-Line fault (LL), Line-to-Line to Ground fault (LLG), and three-phase balanced fault (LLL). As shown in Tab. 3, the fault classification models were trained and evaluated using data sets with varying class distributions.

### 3.5. Placement of PMUs and Sparse Data

PMUs are not installed on all buses of a power system to reduce capital costs [37]. The PSAT toolbox for MATLAB was used for PMU placement [38]. Sixteen buses were identified by the first depth search algorithm and 14 buses by the graph theoretic procedure algorithm for placing the PMUs on the 39 bus test system. Another 9 bus case was considered by placing PMUs on the generator buses of the IEEE 39 bus



(a) LG fault.



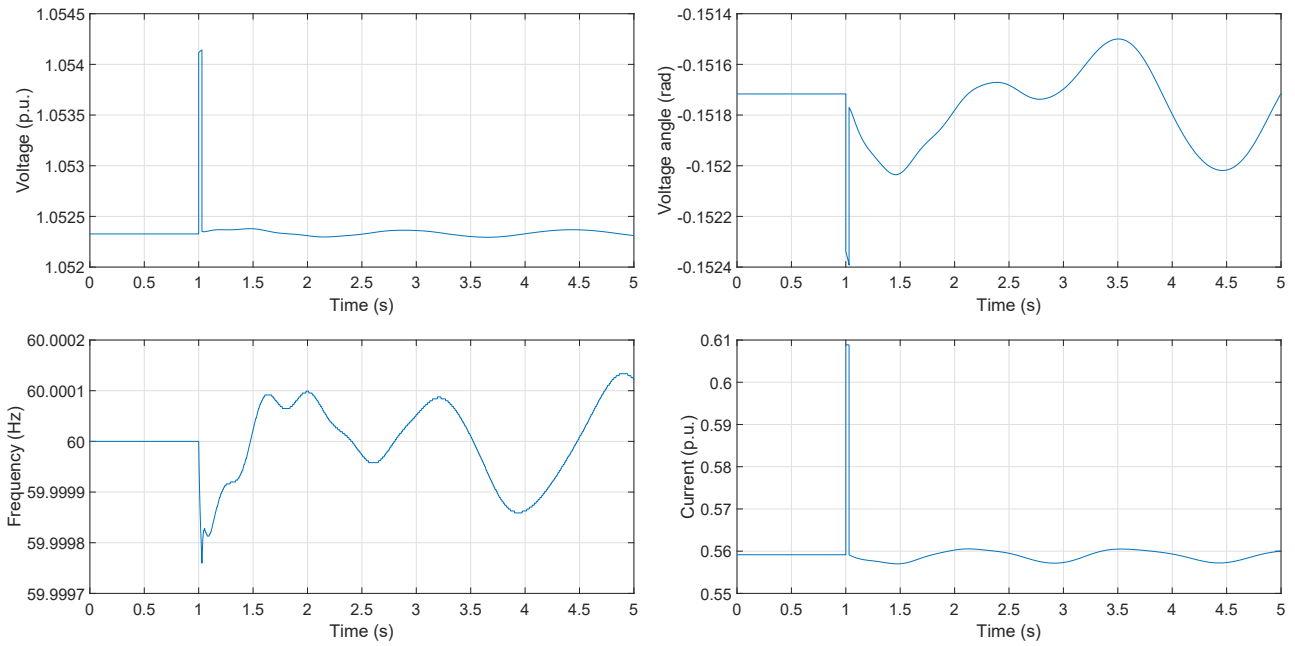
(b) LLL fault.

**Fig. 5:** Voltage, voltage angle, frequency and current signal variations for (a) LG and (b) LLL faults.

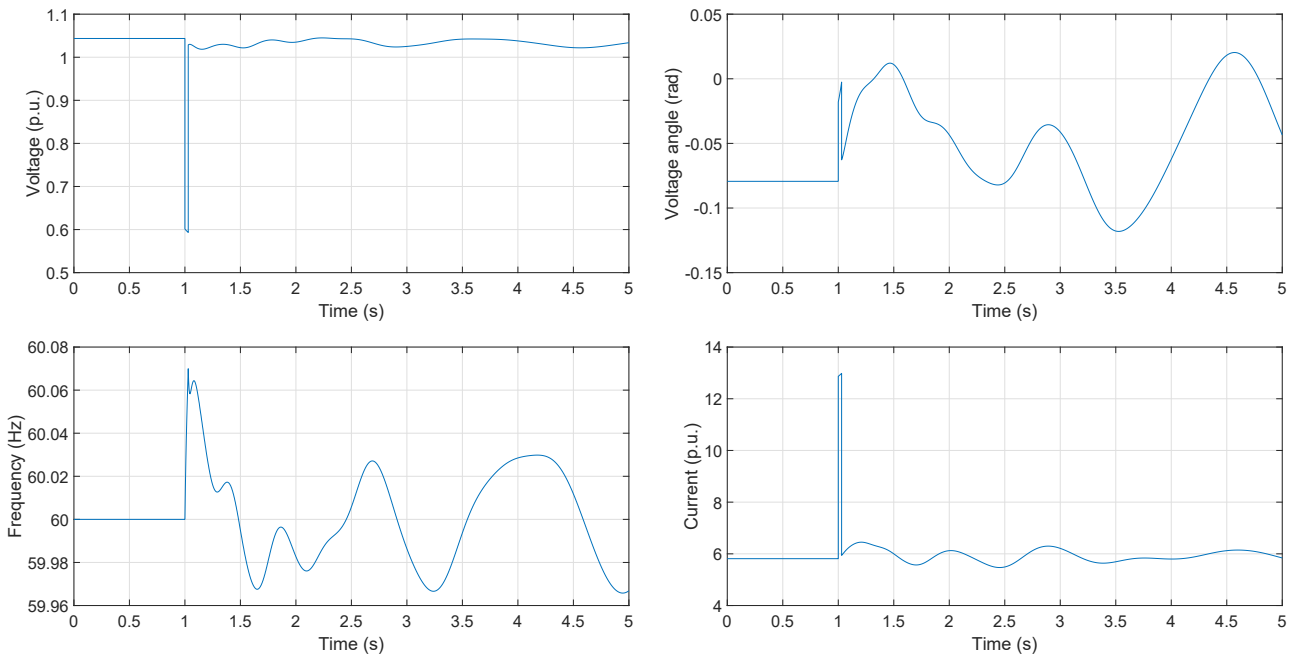
system. The different PMU placement cases considered are:

- PMUs placed on 2, 6, 8, 10, 12, 14, 16, 18, 20, 23, 27, 33, 35, 37, 38, and 39 buses.
- PMUs placed on 4, 8, 16, 28, 31, 32, 33, 34, 35, 36, 37, 38, and 39 buses.
- PMUs placed on 31, 32, 33, 34, 35, 36, 37, 38, and 39 buses.

Datasets were developed with signals from PMUs on, all the buses (39 bus dataset), 16 buses as identified by the first depth search algorithm (16 bus dataset), 14 buses as identified by the graph theoretic procedure (14 bus dataset), and the generator buses (9 bus dataset).



(a) LL fault.



(b) LLG fault.

Fig. 6: Voltage, voltage angle, frequency and current signal variations for (a) LL and (b) LLG faults.

### 3.6. Noisy Data

References [39] and [40] investigated the presence of noise in real-world PMU measurements. In [39], the authors convey that the noise distribution in field PMU data is Gaussian with a Signal-to-Noise Ratio (SNR) of 45 dB or higher. To approximate real-world measurements, white Gaussian noise with SNRs ranging from 30 dB to 60 dB was added to the measurement data sets.

## 4. Results and Discussion

The different feature data sets were derived from the WAMS data set. The performance analysis of the feature data sets with SVM, KNN, DT, BTEC, and ANN classifiers are carried out. The time taken for training, testing, features extraction from the training dataset, features extraction from the testing dataset, and the Accuracy of classification for the different feature data sets are as shown in Tab. 4. The models were trained

**Tab. 4:** List of the performance measures of feature extraction techniques with state-of-the-art classifiers.

FE method	Classifier	Training time (s)	Testing time (s)	Accuracy (%)	Train+FE time (s)	Test+FE time (s)
Wavelet-Energy	SVM	29.672	0.054	92.90	29.895	0.152
	DT	0.046	0.011	93.69	0.269	0.110
	KNN	0.042	0.023	98.95	0.265	0.122
	BTEC	9.266	0.831	98.14	9.489	0.930
	ANN	9.360	0.017	93.13	9.583	0.116
Wavelet-Entropy	SVM	312.330	0.413	66.13	312.593	0.588
	DT	0.049	0.009	38.38	0.224	70.184
	KNN	0.030	0.014	44.58	0.030	0.189
	BTEC	9.725	1.232	40.80	9.725	1.407
	ANN	4.130	0.017	53.38	4.130	0.192
Wavelet Packet Entropy	SVM	1.325	0.039	99.92	28.285	5.699
	DT	0.107	0.025	92.42	27.067	5.685
	KNN	0.028	0.568	99.99	26.988	6.228
	BTEC	1.138	0.108	99.80	28.098	5.714
	ANN	12.768	0.215	66.85	39.728	5.875
Wavelet Packet Energy	SVM	1.438	0.046	99.99	27.913	5.562
	DT	0.106	0.008	94.41	27.027	5.524
	KNN	0.307	0.609	99.86	27.228	6.125
	BTEC	10.690	0.998	99.85	37.611	6.514
	ANN	4.437	0.194	99.76	31.358	5.710
MODWT Energy	SVM	9.637	0.466	62.41	28.359	5.562
	DT	0.137	0.019	61.00	2.382	1.188
	KNN	0.165	0.080	61.80	2.410	1.249
	BTEC	13.524	1.431	61.00	15.769	2.600
	ANN	5.273	0.185	48.21	7.518	1.354
Wavelet Scattering Transform	SVM	38.852	4.897	99.76	41.349	6.051
	DT	2.051	0.014	79.84	4.549	1.168
	KNN	0.246	43.833	99.88	2.744	44.987
	BTEC	78.732	3.734	90.99	81.230	4.888
	ANN	207.140	0.224	96.61	209.638	1.378
Ensemblestatwenergy	SVM	1.979	0.131	99.66	3.069	0.595
	DT	0.13	0.006	60.51	1.220	0.47
	KNN	0.034	0.584	99.76	1.124	1.048
	BTEC	11.83	1.030	97.80	12.920	1.494
	ANN	11.69	0.020	98.53	12.780	0.484
Ensemblestatwentropy	SVM	1.870	0.064	99.36	2.812	0.527
	DT	0.125	0.005	89.68	1.067	0.468
	KNN	0.042	0.430	99.52	0.984	0.893
	BTEC	11.670	1.790	96.40	12.612	2.253
	ANN	20.070	0.013	96.15	21.012	0.476
Ensemblestatwenergywentropy	SVM	1.960	0.131	99.69	3.313	0.770
	DT	0.126	0.006	90.44	1.479	0.645
	KNN	0.044	0.599	99.78	1.397	1.238
	BTEC	11.440	1.021	97.88	12.793	1.660
	ANN	12.860	0.230	97.98	14.213	0.869

and tested on a PC with Intel(R) Core(TM) i7-9750H CPU @ 2.60 GHz , 64-bit operating system, x64-based processor, and 32 GB RAM.

The wavelet packet transform-based features showed superior performance in terms of accuracy. The computational efficiency of this method is poor as the time taken for feature extraction is very high and this increases the time to train and test the models.

Wavelet scattering transform coefficients features are correctly classified with an accuracy of 99.76 % by the SVM classifier and 99.88 % by the KNN classifier. The time to train and test the WST feature dataset is very high.

The ensemble methods showed superior performance in terms of computational time as well as accuracy.

KNN classifier classified Ensemblestatenergy feature set with an accuracy of 99.76 % within 1.048 s and Ensemblestatenergyentropy feature dataset with an accuracy of 99.78 % within 1.238 s. The classification accuracy of SVM with Ensemblestatenergy and Ensemblestatenergyentropy feature data sets were above 99.66 % with a testing time of 0.59 s.

The Ensemblestatenergyentropy method was used to extract features from the 16 bus, 14 bus, and the 9 bus data sets with Gaussian noise of SNR ranging from 30 dB to 60 dB. The accuracy of classification by the models trained with sparse and noisy measurement data sets are as in Fig. 10. The accuracy of classification is above 96 % for all the models with a 40 dB noise level. This validates the efficacy of the ensemble features for fault classification using WAMS data.

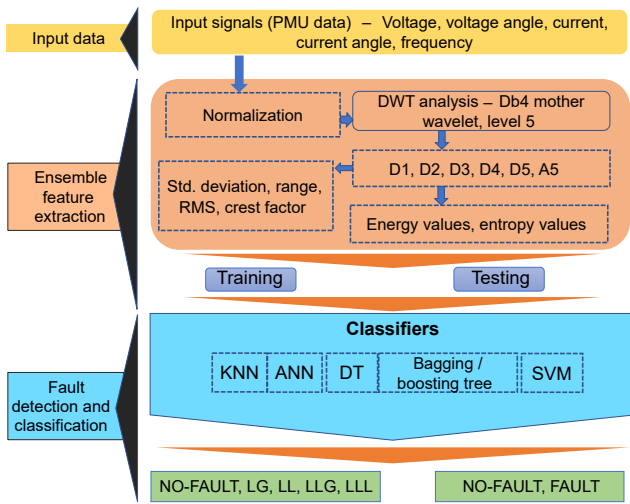


Fig. 7: Process flow for detecting and classifying faults.

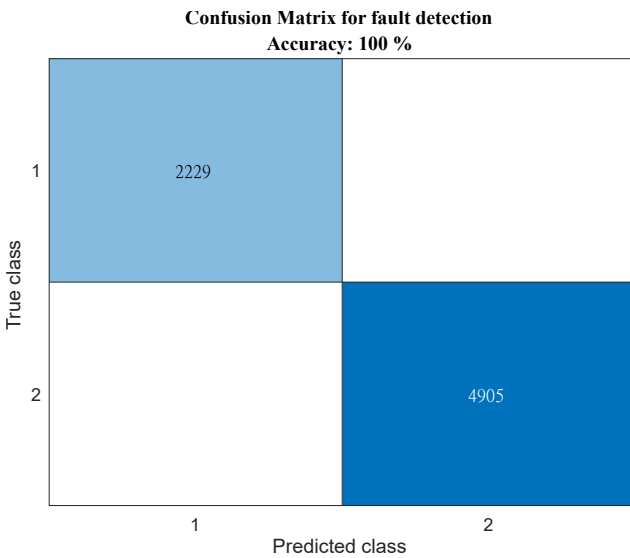


Fig. 8: Confusion matrix for fault detection with Ensemblestatenergyentropy feature data set and SVM.

All the feature data sets were classified with 100 % accuracy by the fault detection models. The confusion matrix for the fault detection and classification with the Ensemblestatenergyentropy feature data set and SVM classifier are shown in Fig. 8 and Fig. 9.

### 5. Conclusion

The performance of a machine learning classifier is predominantly dependent on the input data. The feature data set provided as input has a significant impact on the performance of the classifier model. The proposed ensemble feature dataset comprises statistical features of wavelet coefficients, energy, and the entropy values of the wavelet coefficients. The performance of this ensemble feature method is validated and found

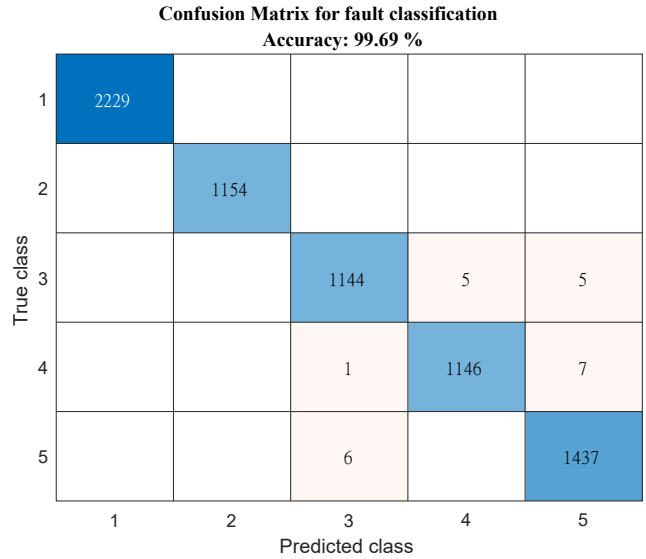


Fig. 9: Confusion matrix for fault classification with Ensemblestatenergyentropy feature data set and SVM.

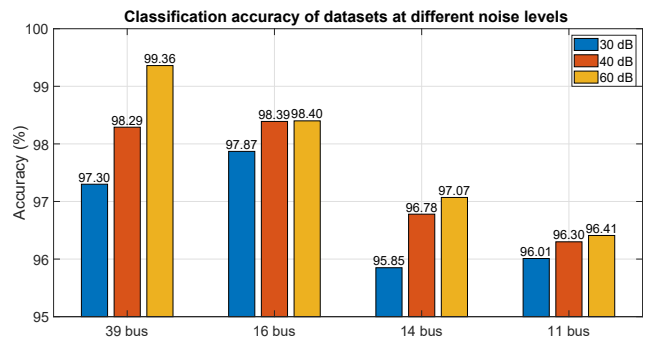


Fig. 10: Performance of different datasets with noise levels from SNR 30 dB to 60 dB.

to be superior when compared to wavelet entropy, wavelet energy, wavelet packet entropy, energy values of MODWT coefficients, and wavelet scattering transform coefficients.

For today’s complex power grid with the dispersed generation, fault analysis methodologies that may offer power system operators with a large area situation awareness viewpoint are needed. When creating and implementing these intelligent models for fault diagnosis on the smart grid, the computational efficiency of the machine learning models should be prioritised. The presented ensemble features data set for fault classification was categorised by the SVM classifier with an accuracy of 99.69 % in 0.56 s. Since the latency is within the acceptable range for backup protection of power transmission lines, these models can serve as critical components of power system backup protection systems for speedy fault resolution.

## Acknowledgment

This work was supported by the Government of Kerala, Higher Education Fellowship Program.

## Author Contributions

A.H. carried out the simulation, development of models, experiments and wrote the manuscript. P.A contributed to the analysis of the results, manuscript preparation and supervised the work. J.M.V supported the supervision of the work and reviewed the manuscript.

## References

- [1] LI, F., W. QIAO, H. SUN, H. WAN, J. WANG, Y. XIA, Z. XU and P. ZHANG. Smart Transmission Grid: Vision and Framework. *IEEE Transactions on Smart Grid*. 2010, vol. 1, iss. 2, pp. 168–177. ISSN 1949-3061. DOI: 10.1109/TSG.2010.2053726.
- [2] RIVAS, A. E. L. and T. ABRAO. Faults in smart grid systems: Monitoring, detection and classification. *Electric Power Systems Research*. 2020, vol. 189, iss. 1, pp. 1–26. ISSN 1873-2046. DOI: 10.1016/j.epsr.2020.106602.
- [3] BHUIYAN, S. M. A., J. F. KHAN and G. V. MURPHY. Big data analysis of the electric power PMU data from smart grid. In: *SoutheastCon 2017*. Concord: IEEE, 2017, pp. 1–5. ISBN 978-1-5386-1539-3. DOI: 10.1109/SECON.2017.7925277.
- [4] BISWAL, M., S. M. BRAHMA and H. CAO. Supervisory Protection and Automated Event Diagnosis Using PMU Data. *IEEE Transactions on Power Delivery*. 2016, vol. 31, iss. 4, pp. 1855–1863. ISSN 1937-4208. DOI: 10.1109/TPWRD.2016.2520958.
- [5] TIRNOVAN, R.-A. and M. CRISTEA. Advanced techniques for fault detection and classification in electrical power transmission systems: An overview. In: *2019 8th International Conference on Modern Power Systems (MPS)*. Cluj-Napoca: IEEE, 2019, pp. 1–10. ISBN 978-1-7281-0750-9. DOI: 10.1109/MPS.2019.8759695.
- [6] PHADKE, A. G., P. WALL, L. DING and V. TERZIJA. Improving the performance of power system protection using wide area monitoring systems. *Journal of Modern Power Systems and Clean Energy*. 2016, vol. 4, iss. 3, pp. 319–331. ISSN 2196-5420. DOI: 10.1007/s40565-016-0211-x.
- [7] DASGUPTA, A., S. NATH and A. DAS. Transmission Line Fault Classification and Location Using Wavelet Entropy and Neural Network. *Electric Power Components and Systems*. 2012, vol. 40, iss. 15, pp. 1676–1689. ISSN 1532-5016. DOI: 10.1080/15325008.2012.716495.
- [8] MAJD, A. A., H. SAMET and T. GHANBARI. k-NN based fault detection and classification methods for power transmission systems. *Protection and Control of Modern Power Systems*. 2017, vol. 2, iss. 1, pp. 1–11. ISSN 2367-0983. DOI: 10.1186/s41601-017-0063-z.
- [9] EKICI, S. Support Vector Machines for classification and locating faults on transmission lines. *Applied Soft Computing*. 2012, vol. 12, iss. 6, pp. 1650–1658. ISSN 1872-9681. DOI: 10.1016/j.asoc.2012.02.011.
- [10] SHAIK, A. G. and R. R. V. PULIPAKA. A new wavelet based fault detection, classification and location in transmission lines. *International Journal of Electrical Power & Energy Systems*. 2015, vol. 64, iss. 1, pp. 35–40. ISSN 1879-3517. DOI: 10.1016/j.ijepes.2014.06.065.
- [11] GOPAKUMAR, P., M. J. B. REDDY and D. K. MOHANTA. Transmission line fault detection and localisation methodology using PMU measurements. *IET Generation, Transmission & Distribution*. 2015, vol. 9, iss. 11, pp. 1033–1042. ISSN 1751-8695. DOI: 10.1049/iet-gtd.2014.0788.
- [12] ROY, N. and K. BHATTACHARYA. Detection, Classification, and Estimation of Fault Location on an Overhead Transmission Line Using S-transform and Neural Network. *Electric Power Components and Systems*. 2015, vol. 43, iss. 4, pp. 461–472. ISSN 1532-5016. DOI: 10.1080/15325008.2014.986776.
- [13] MOHAMAD, N. Z., A. F. ABIDIN and I. MUSIRIN. Intelligent Power Swing Detection Scheme to Prevent False Relay Tripping Using S-Transform. *International Journal of Emerging Electric Power Systems*. 2014, vol. 15, iss. 3, pp. 291–298. ISSN 1553-779X. DOI: 10.1515/ijeeps-2013-0107.
- [14] ANAND, A. and S. AFFIJULLA. Hilbert-Huang transform based fault identification and classification technique for AC power transmission line protection. *International Transactions on Electrical Energy Systems*. 2020, vol. 30, iss. 10, pp. 1–15. ISSN 2050-7038. DOI: 10.1002/2050-7038.12558.

- [15] SOMAN, K. P. and K. I. RAMACHANDRAN. *Insight into Wavelets From Theory to Practice*. 2nd ed. New Delhi: Prentice Hall of India Private Limited, 2004. ISBN 978-81-203-2650-7.
- [16] CHAOVALIT, P., A. GANGOPADHYAY, G. KARABATIS and Z. CHEN. Discrete wavelet transform-based time series analysis and mining. *ACM Computing Surveys*. 2011, vol. 43, iss. 2, pp. 1–37. ISSN 1557-7341. DOI: 10.1145/1883612.1883613.
- [17] GAO, R. X. and R. YAN. Wavelet Packet Transform. In: *Wavelets*. 1st ed. Boston: Springer, 2011, pp. 69–81. ISBN 978-1-4419-1545-0.
- [18] JNANESWAR, K., B. MALLIKARJUNA, S. DEVARAJ, D. S. ROY, M. J. B. REDDY and D. K. MOHANTA. A real-time DWT and traveling waves-based multi-functional scheme for transmission line protection reinforcement. *Electrical Engineering*. Springer Berlin Heidelberg. 2021, vol. 103, iss. 2, pp. 965–981. ISSN 1432-0487. DOI: 10.1007/s00202-020-01117-0.
- [19] HAQ, E. U., H. JIANJUN, K. LI, F. AHMAD, D. BANJERDPONGCHAI and T. ZHANG. Improved performance of detection and classification of 3-phase transmission line faults based on discrete wavelet transform and double-channel extreme learning machine. *Electrical Engineering*. 2021, vol. 103, iss. 2, pp. 953–963. ISSN 1432-0487. DOI: 10.1007/s00202-020-01133-0.
- [20] HASABE, R. P. and A. P. VAIDYA. Detection and classification of faults on 220 KV transmission line using wavelet transform and neural network. *International Journal of Smart Grid and Clean Energy*. 2014, vol. 3, iss. 3, pp. 283–290. ISSN 2373-3594. DOI: 10.12720/sgce.3.3.283-290.
- [21] PATEL, B., P. BERA and B. SAHA. Wavelet Packet Entropy and RBFNN Based Fault Detection, Classification and Localization on HVAC Transmission Line. *Electric Power Components and Systems*. 2018, vol. 46, iss. 1, pp. 15–26. ISSN 1532-5016. DOI: 10.1080/15325008.2018.1431817.
- [22] ANANTHAN, S. N., R. PADMANABHAN, R. MEYUR, B. MALLIKARJUNA, M. J. B. REDDY and D. K. MOHANTA. Real-time fault analysis of transmission lines using wavelet multi-resolution analysis based frequency-domain approach. *IET Science, Measurement & Technology*. 2016, vol. 10, iss. 7, pp. 693–703. ISSN 1751-8830. DOI: 10.1049/iet-smt.2016.0038.
- [23] COSTA, F. B., B. A. SOUZA and N. S. D. BRITO. Real-time classification of transmission line faults based on Maximal Overlap Discrete Wavelet Transform. In: *PES T&D 2012*. Orlando: IEEE, 2012, pp. 1–8. ISBN 978-1-4673-1935-5. DOI: 10.1109/TDC.2012.6281684.
- [24] JAMEHBOZORG, A. and S. M. SHAHRTASH. A Decision Tree-Based Method for Fault Classification in Double-Circuit Transmission Lines. *IEEE Transactions on Power Delivery*. 2010, vol. 25, iss. 4, pp. 2184–2189. ISSN 1937-4208. DOI: 10.1109/TPWRD.2010.2050911.
- [25] MISHRA, P. K., A. YADAV and M. PAZOKI. A Novel Fault Classification Scheme for Series Capacitor Compensated Transmission Line Based on Bagged Tree Ensemble Classifier. *IEEE Access*. 2018, vol. 6, iss. 1, pp. 27373–27382. ISSN 2169-3536. DOI: 10.1109/ACCESS.2018.2836401.
- [26] HARISH, A. and M. V. JAYAN. Classification of Power Transmission Line Faults Using an Ensemble Feature Extraction and Classifier Method. In: *Inventive Communication and Computational Technologies: Proceedings of ICI-CCT 2020*. Pachal: Springer, 2020, pp. 417–427. ISBN 978-981-15-7345-3. DOI: 10.1007/978-981-15-7345-3\_35.
- [27] PANDEY, S., A. K. SRIVASTAVA and B. G. AMIDAN. A Real Time Event Detection, Classification and Localization Using Synchrophasor Data. *IEEE Transactions on Power Systems*. 2020, vol. 35, iss. 6, pp. 4421–4431. ISSN 1558-0679. DOI: 10.1109/tpwrs.2020.2986019.
- [28] YOUSEFINEZHAD, M., S. RAHIMI, M. ALIREZAIEAN, M. VALIZADEH and H. A. ABYANEH. A new simple and accurate method for fault detection in wide area protection. *Electric Power Systems Research*. 2022, vol. 213, iss. 1, pp. 1–17. ISSN 1873-2046. DOI: 10.1016/j.epsr.2022.108775.
- [29] CRESPO, D. L. C. and M. MORETO. New technique for fault location in distribution systems using sincrophasor voltages. *Electric Power Systems Research*. 2022, vol. 212, iss. 1, pp. 1–9. ISSN 1873-2046. DOI: 10.1016/j.epsr.2022.108485.
- [30] VEERASAMY, V., N. I. A. WAHAB, M. L. OTHMAN, S. PADMANABAN, K. SEKAR, R. RAMACHANDRAN, H. HIZAM, A. VINAYAGAM and M. Z. ISLAM. LSTM Recurrent Neural Network Classifier for High Impedance Fault Detection in Solar PV Integrated Power System. *IEEE Access*. 2021, vol. 9, iss. 1, pp. 32672–32687. ISSN 2169-3536. DOI: 10.1109/ACCESS.2021.3060800.

- [31] SWAIN, K. B., S. S. MAHATO and M. CHERUKURI. Expeditious Situational Awareness-Based Transmission Line Fault Classification and Prediction Using Synchronized Phasor Measurements. *IEEE Access*. 2019, vol. 7, iss. 1, pp. 168187–168200. ISSN 2169-3536. DOI: 10.1109/ACCESS.2019.2954337.
- [32] DGHAIS, A. A. A. and M. T. ISMAIL. A Comparative Study between Discrete Wavelet Transform and Maximal Overlap Discrete Wavelet Transform for Testing Stationarity. 2013. DOI: 10.5281/zenodo.1089273.
- [33] SAYDJARI, A. K. and D. P. FINKBEINER. Equivariant Wavelets: Fast Rotation and Translation Invariant Wavelet Scattering Transforms. *IEEE Transactions on Pattern Analysis and Machine Intelligence*. 2023, vol. 45, iss. 2, pp. 1716–1731. ISSN 1939-3539. DOI: 10.1109/TPAMI.2022.3165730.
- [34] BRUNI, V., M. L. CARDINALI and D. VITULANO. An MDL-Based Wavelet Scattering Features Selection for Signal Classification. *Axioms*. 2022, vol. 11, iss. 8, pp. 1–12. ISSN 2075-1680. DOI: 10.3390/axioms11080376.
- [35] LIU, Z., G. YAO, Q. ZHANG, J. ZHANG and X. ZENG. Wavelet Scattering Transform for ECG Beat Classification. *Computational and Mathematical Methods in Medicine*. 2020, vol. 2020, iss. 1, pp. 1–11. ISSN 1748-6718. DOI: 10.1155/2020/3215681.
- [36] Electric Grid Test Cases: IEEE 39-Bus System. In: *Texas A&M University Electric Grid Datasets* [online]. 2023. Available at: <https://electricgrids.engr.tamu.edu/electric-grid-test-cases/ieee-39-bus-system/>.
- [37] YUILL, W., A. EDWARDS, S. CHOWDHURY and S. P. CHOWDHURY. Optimal PMU placement: A comprehensive literature review. In: *2011 IEEE Power and Energy Society General Meeting*. Detroit: IEEE, 2011, pp. 1–8. ISBN 978-1-4577-1002-5. DOI: 10.1109/PES.2011.6039376.
- [38] MILANO, F. An open source power system analysis toolbox. *IEEE Transactions on Power Systems*. 2005, vol. 20, iss. 3, pp. 1199–1206. ISSN 1558-0679. DOI: 10.1109/TPWRS.2005.851911.
- [39] BROWN, M., M. BISWAL, S. BRAHMA, S. J. RANADE and H. CAO. Characterizing and quantifying noise in PMU data. In: *2016 IEEE Power and Energy Society General Meeting (PESGM)*. Boston: IEEE, 2016, pp. 1–5. ISBN 978-1-5090-4168-8. DOI: 10.1109/PESGM.2016.7741972.
- [40] BHANDARI, A., H. YIN, Y. LIU, W. YAO and L. ZHAN. Real-Time Signal-to-Noise Ratio Estimation by Universal Grid Analyzer. In: *2019 International Conference on Smart Grid Synchronized Measurements and Analytics (SGSMA)*. College Station: IEEE, 2019, pp. 1–6. ISBN 978-1-7281-1607-5. DOI: 10.1109/SGSMA.2019.8784676.

## About Authors

**Ani HARISH** (corresponding author) was born in Kerala, India. She received B.Tech. degree in electrical engineering from Mahatma Gandhi University, Kerala, India, in 1997, and M.Tech. degree in power systems from Kerala University, India, in 2000. She is currently pursuing Ph.D. degree from APJ Abdul Kalam Technological University, Kerala, India. Her research interests include wide area measurements, wide area monitoring and control of power systems, and artificial intelligence applications in power systems.

**Prince ASOK** was born in Kerala, India. He received B.Tech. degree in electrical engineering from Kerala University, India, in 1996, M.Tech. degree in energy studies in 2005 and Ph.D. in power systems in 2012 from the Indian Institute of Technology, Delhi, India. He has been in academia for 21 years and is currently serving as a professor of electrical engineering at Rajiv Gandhi Institute of Technology, Kerala, India. His research interests include power systems, renewable energy systems, wide area measurements, electric vehicles and signal processing applications in power systems, power electronics applications in power systems, and artificial intelligence applications in power systems.

**Jayan Madasseril VASUDEVAN** was born in Kerala, India. He received B.Tech. degree in electrical engineering from Kerala University, India, in 1987, and M.E. degree in control systems from Bharathiar University, Coimbatore, India, in 2003, and Ph.D. in high voltage engineering from the Indian Institute of Science, Bangalore, India, in 2009. He retired as a professor of Electrical Engineering in 2021 from Government College of Engineering, Thrissur, Kerala, India. His current research interests include high voltage engineering, solid pollution control, wide area monitoring and control of power systems, and power quality enhancement in grid integrated power systems.